Desalination and Water Treatment
www.deswater.com
doi: 10.5004/dwt.2023.29567

294 (2023) 213–224
May

TiO_2 nanoparticles grafted with 2,4-dinitrophenylhydrazine as a new adsorbent in efficient removal of formaldehyde from aqueous solution

Zahra Hejri[a,*], Ali Hasani[b]

[a]*Department of Chemical Engineering, Quchan Branch, Islamic Azad University, Quchan, Iran, 94791-76135, email: za.hejri@iau.ac.ir*
[b]*Department of Chemical Engineering, Ferdowsi University of Mashhad, Iran, email: ali.hasani@njit.edu*

Received 16 January 2023; Accepted 16 April 2023

ABSTRACT

A novel adsorbent prepared by the immobilization of 2,4-dinitrophenylhydrazine (DNPH) on TiO_2 nanoparticles has been investigated for the removal of formaldehyde from aqueous solutions. Sodium dodecyl sulfate (SDS) surfactant was used to improve the DNPH grafting to the TiO_2 surface. Isotherm modeling revealed that the Langmuir equation could better describe the adsorption of formaldehyde onto the TiO_2/SDS/DNPH and the maximum adsorption capacity obtained was 51.282 mg/g. The equilibrium parameter (R_L) indicated that TiO_2/SDS/DNPH nanocomposites are useful for the removal of formaldehyde from aqueous solutions. Kinetic studies showed the best applicability of the pseudo-first-order model. It was found that the adsorption rate is rapid at the initial stages and reaches equilibrium after 245 min. According to the adsorption thermodynamics, $\Delta H°$, $\Delta G°$, and $\Delta S°$ were calculated as –26.1, –5.6, and –63.2 (kJ/mol), respectively. Negative values obtained for thermodynamic parameters show that the reaction is exothermic and spontaneous at room temperature. Adsorption–desorption studies indicated that the prepared adsorbent kept its adsorption efficiencies constant over 5 cycles. The best conditions for TiO_2/SDS/DNPH nanocomposites to remove 96.2% formaldehyde were an adsorbent dosage of 1.1 g/L, a pH of 7.424 and a contact time of 183.290 min.

Keywords: Titanium dioxide; 2,4-Dinitrophenylhydrazine; Formaldehyde; Aqueous solution; Adsorption

1. Introduction

Formaldehyde (HCHO) is a toxic compound, with a lethal dose of 500 mg/kg [1]. Recently, the International Agency for Research on Cancer and the National Toxicology Program have designated formaldehyde as a human carcinogen [2]. It has wide applications in various industries, including the production of polymers, adhesives, sponges, detergents, preservatives, explosive materials, wood processing, textiles, leather, and cosmetics [3]. Formaldehyde is found in wastewater in monomeric form, as well as its derivatives such as ether, urea, phenolic condensates, and it forms composite complexes with resins, phenols, and many other chemicals [4]. Therefore, to minimize the harmful effects of formaldehyde, it should be removed effectively from wastewater.

Several methods for formaldehyde removal have been proposed, such as membrane separation [5], advanced oxidation processes [6], biological [1,4,7,8] and electrocoagulation [9], which are often costly and complex with low efficiency and by-products. Adsorption has been shown to be the most efficient method for the removal of pollutants from aqueous solutions [9–13]. Salman et al. [14] had studied the adsorption of formaldehyde on bentonite and kaolin in batch mode. They concluded that kaolin and bentonite have good potential as adsorbents to remove toxic organic pollutants such as formaldehyde from water. Ryu et al. [15] had examined urea/nitric acid co-impregnated pitch-based activated carbon

* Corresponding author.

fibers as adsorbents for the removal of low-concentration formaldehyde gas from dry and humid atmospheres. Na et al. [16] studied the formaldehyde adsorption performance of materials with particular emphasis on advanced materials (e.g., carbon nanotubes, metal–organic frameworks, graphene oxides, and porous organic polymers) and their modified forms compared to conventional sorbents (e.g., zeolite). Nanosorbents have emerged as a new area of research with potential application, due to their large surface areas, high number of surface-active sites, easy synthesis, and rapid absorption. However, most of the used adsorbents have not succeeded in effectively removing formaldehyde, especially at high concentrations [17].

Among all nanoscale metal oxides, titanium dioxide nanocrystals (TiO_2) have a high potential for environmental applications due to their physical and chemical stability, relatively lower cost, nontoxicity, resistance to corrosion, and stable colloidal suspension [18–22]. Furthermore, TiO_2 can be recovered from various effluents and can be reused as a sorbent in the elimination of pollutants from air and water [23–26]. Anatase nanoparticles have a higher sorption capacity compared to other phases of TiO_2 [27,28]. Formaldehyde molecules can be adsorbed on the hydroxyl groups on the surface of TiO_2 by hydrogen bonding [29]; however, since amine groups have been proven to improve formaldehyde adsorption through their reaction that produces imine [30,31], it is anticipated that impregnation of TiO_2 with amino-containing compounds can improve its removal capacity for formaldehyde due to the cooperation of physical adsorption and the increased chemical interaction between amino groups on the surface of the adsorbent and formaldehyde molecules. Although the adsorption and photocatalytic oxidation of gaseous formaldehyde on pure TiO_2 have been studied [29], some important aspects of the removal of formaldehyde from water by adsorption on grafted TiO_2 nanoparticles are still poorly understood. One of the compounds with a strong affinity for formaldehyde is 2,4-dinitrophenylhydrazine [32,33], which can be used with TiO_2 as a new adsorbent for the efficient removal of formaldehyde from aqueous solutions. In this study, we synthesized 2,4-dinitrophenylhydrazine grafted TiO_2 nanocrystals and investigated their application in the removal of formaldehyde from aqueous solutions. The effect of pH and absorbent dosage on adsorption efficiency was investigated, as well as on adsorption kinetics, thermodynamics, and isotherms.

2. Materials and methods

2.1. Materials

The nano-TiO_2 powder (anatase-phase crystal structure with an average particle size of approximately 25 nm) was supplied by Nanolin, Germany. Formalin solution (37 wt.% of formaldehyde), ammonium acetate (98% purity), acetic acid (96% purity); acetylacetone (99% purity), 2,4-dinitrophenylhydrazine (99% purity), and sodium dodecyl sulfate were purchased from Merck, Germany.

2.2. Preparation and characterization of adsorbent

The TiO_2/SDS/DNPH nanocomposite was prepared by immobilizing 2,4-dinitrophenylhydrazine on TiO_2 nanoparticles coated with anionic sodium dodecyl sulfate surfactant as a grafting agent between TiO_2 and 2,4-dinitrophenylhydrazine (DNPH) [17,32]. DNPH was used as an agent to form amine groups on the surface of TiO_2. First, 2.0 g TiO_2 nanoparticles were suspended in 50 mL deionized water. Then 100 mg of sodium dodecyl sulfate (SDS) and 20 mL of DNPH solution (0.9 g of DNPH in a concentrated solution of hydrochloric acid and acetonitrile) were added. The solution was stirred at 60°C for 3 h and the excess solvent evaporated under vacuum. The remaining solid phase was washed with deionized water and, after drying, kept in a sealed container for subsequent use.

As in our previous research [34], the morphology of the nanoparticles was studied using the Cambridge S360 scanning electron microscopy (SEM) equipped with an Oxford energy-dispersive X-ray spectroscopy (EDX). All images were taken with an operating voltage of 30 kV and 200; 500; 1,000 and 2,000 magnifications. Specimens were sputter-coated with gold in a Quorum Sputter Coater Model Q150R ES. A closer look at the shape, size, and arrangement of the nanostructure adsorbent was carried out by Philips transmission electron microscopy (TEM) model CM120. The X-ray diffraction analysis (XRD) was performed at an angular range of 5°–70° (2θ) with a step size of 2θ = 0.02° in Philips Analytical X-Ray diffractometer model X'Pert PW 3040/60 using a CuK_α radiation (λ = 1.5406 nm), 40 kV, and 30 mA. The diffractometer was equipped with 1° divergence slit and a 0.1 mm receiving slit. Fourier-transform infrared spectroscopy (FTIR) was performed using the Thermo Nicolet Apparatus Model Avatar 370, made in the USA. All the peaks were obtained in the range of 4,000 to 400 cm^{-1} for modified and unmodified nanoadsorbent.

2.3. Experiments design

The response surface method (RSM) and the central composite design (CCD) were used for experiment design, data analysis, and to determine the effect of various process parameters such as contact time, pH, and adsorbent dosage on adsorption efficiency. Three levels for each parameter were considered with 20 runs containing 8 factorial points, 6 central points, and 6 axial points [35]. The levels of factors were selected according to preliminary tests. Design–Expert software version 10 was applied for the analysis of variance (ANOVA), with 0.05 significance level. The optimal value for each of the three parameters was determined according to the responses obtained. Factors under study along with their levels are summarized in Table 1.

2.4. Adsorption studies

Adsorption experiments were conducted discontinuously in the presence of nitrogen (to prevent oxidation). Certain concentrations of formaldehyde at a specific contact time and pH were subjected to different amounts of adsorbent, according to the design of the relevant experiments [36]. Aqueous formaldehyde solution was stirred on a magnetic stirrer at 1,000 rpm to allow transfer of the pollutant onto the adsorbent. The adsorbent was separated by centrifuge at 15,000 rpm for 15 min and residual formaldehyde concentration in aqueous solution was determined through

formaldehyde reaction with Hantzsch reagent based on Nash method [37]. The adsorption efficiency and adsorbed amount of formaldehyde per unit weight of adsorbent at time t, q_t (mg/g), were calculated as:

$$\text{Adsorption Efficiency}(\%) = \frac{C_0 - C_t}{C_0} \times 100 \quad (1)$$

$$q_t = \frac{(C_0 - C_t)V}{W} \quad (2)$$

where C_0 and C_t (mg/L) are the initial and time t concentrations of formaldehyde, respectively. V (L) is the volume of the solution, and W (g) is the mass of adsorbent used. Adsorption equilibrium tests were performed by adding 1.1 g/L of TiO_2/SDS/DNPH at pH 7.4 (the optimum conditions) to an aqueous solution containing 100, 200, 300, 400 and 500 ppm formaldehyde. The samples were stirred to reach equilibrium, and then the solution was analyzed for residual formaldehyde. q_e (mg/g), were computed as:

$$q_t = \frac{(C_0 - C_e)V}{W} \quad (3)$$

where C_e (mg/L) denotes the formaldehyde concentration at equilibrium.

2.5. Regeneration and reusability of adsorbent

To evaluate the possibility of recycling the adsorbent, the regeneration process of TiO_2/SDS/DNPH nanocomposites was conducted using 1 M sodium hydroxide, 0.5 M acetic acid, and water steam as adsorbent recovery solutions [38]. For this purpose, 1 g of TiO_2/SDS/DNPH nanocomposites, previously saturated with formaldehyde, were agitated with 50 mL of recovery solution and subjected to hot steam for 3 h, followed by ultrasonication for 5 min to desorb the formaldehyde from them. Adsorbents were separated by centrifugation and then washed with deionized water for 5 min. The formaldehyde removal performance of the regenerated adsorbent was measured in a new adsorption experiment. This adsorption–desorption cycle was repeated five times to test the reusability of the adsorbents.

Table 1
Factors under study along with their levels

Factor	Level	
	Low	High
A: Contact time (min)	60	210
B: pH	4	10
C: Adsorbent dosage (g/L)	0.5	1.5

3. Results and discussion

3.1. Morphological properties

The morphologies and microstructures of the prepared samples were observed by SEM and TEM images. SEM micrographs of titanium dioxide nanoparticles and their modified forms are shown in Fig. 1a and b. The micrographs, taken from the surface of samples, illustrate that particles are largely spherical, and the modified particles are slightly larger than the unmodified particles. The SEM results reveal that the resulting nanocomposites are spherical with an average diameter of 70–80 nm and no agglomeration. The larger size of the TiO_2/SDS/DNPH nanoparticles indicates a good grafting of the TiO_2 nanoparticles with the modifier factor (Fig. 1b), which has been reported recently by Kianpour et al. [39]. TEM images of SDS-coated TiO_2 modified with DNPH (Fig. 2) reveal that the average diameter of the prepared nanoparticles was below 100 nm, consistent with the SEM images. Furthermore, the coated core is visible, showing a good coating of TiO_2 nanoparticles with SDS and grafting with DNPH. Indeed, SDS can bind to specific facets of the TiO_2, and then the TiO_2 core is coated with a monolayer of SDS. This SDS monolayer can hold the surface energy of the TiO_2 nanocrystal facets. Attached SDS reduces the total surface energy of TiO_2 nanocrystals by blocking the high energy facets [40,41].

3.2. Structural properties

The elemental composition of the prepared TiO_2/SDS/DNPH nanocomposite was identified by an EDX coupled

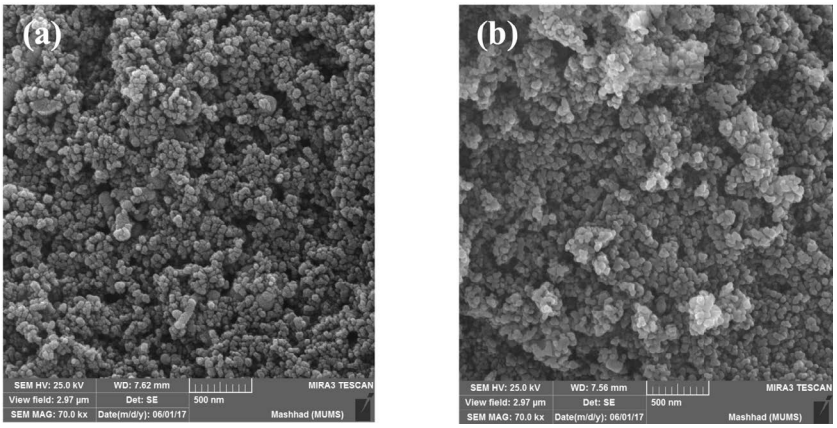

Fig. 1. Scanning electron microscopy images of (a) titanium dioxide nanoparticles and (b) TiO_2/SDS/DNPH nanocomposites.

with SEM. The elemental analysis data (Fig. 3) confirmed the presence of carbon, titanium, oxygen, sodium, nitrogen, sulfur, and chlorine elements in the composition of the compound. The presence of some oxygen in the composition is not surprising, since the occurrence of partial oxidation is inevitable [42]. The presence of some nitrogen was expected to enhance the absorption capacity of TiO_2 for formaldehyde removal from water. The role of nitrogen in improving the absorption capacity of TiO_2 was also reported recently by Li et al. [43].

The crystal structure of the TiO_2 nanoparticles and the TiO_2/SDS/DNPH nanocomposites was determined using XRD with 2θ diffraction angles varying from 5° to 70° (Fig. 4). TiO_2 exhibits a characteristic sharp peak at 2θ = 25.402° corresponding to the plane spacing (*d*-spacing) of 0.351 nm [18,21]. Furthermore, the main diffraction peaks at (101), (103), (004), (112), (200) and (204) by comparison with the Joint Committee on Powder Diffraction Standards (JCPDS card, file No. 21–1272), are indexed to TiO_2 anatase phase. Since the compounds grafted with TiO_2 are organic, the XRD pattern of the TiO_2/SDS/DNPH nanocomposite has the same pattern as for TiO_2 [18].

FTIR was used to characterize the modification of the surface amine of the prepared TiO_2/SDS/DNPH samples (Fig. 5). In the nano-TiO_2 spectrum, a strong and broad absorption band at 3,430.52 cm^{-1} shows a large amount of –OH on the nano-TiO_2 surface. The absorption band at 1,629.16 cm^{-1} is related to the Ti–OH bending vibration, and the absorption band at 713.06 cm^{-1} indicates the Ti–O–Ti stretching vibration [44,45]. A comparison between the FTIR spectra of the TiO_2/SDS/DNPH nanocomposite and the spectra of the TiO_2 nanoparticles indicates that the surface-modified TiO_2 nanoparticles contained an N–H functional group due to the immobilization procedure. In the TiO_2/SDS/DNPH spectrum, the strong and broad band at 3,200–3,500 cm^{-1} is referred to –OH stretching vibrations related to water (which should be in the range of 3,200–3,500 cm^{-1}) or N–H symmetric stretching vibrations (which should be in the range of

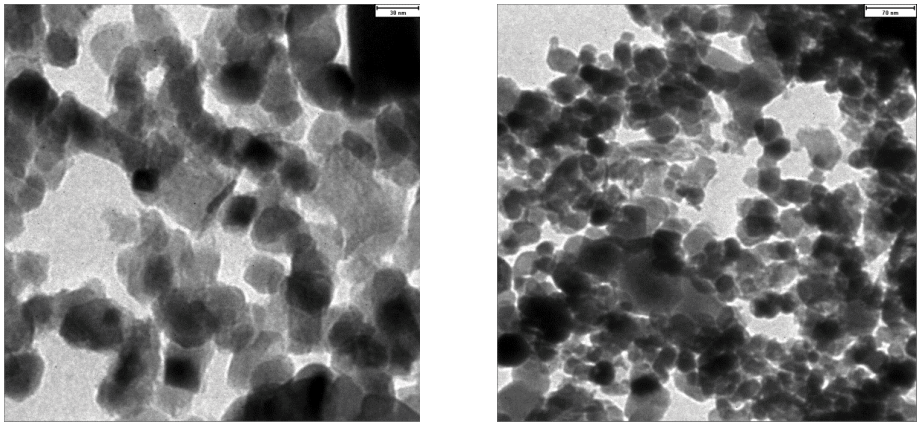

Fig. 2. Transmission electron microscopy images of TiO_2/SDS/DNPH nanocomposite (scale bar: 70 nm).

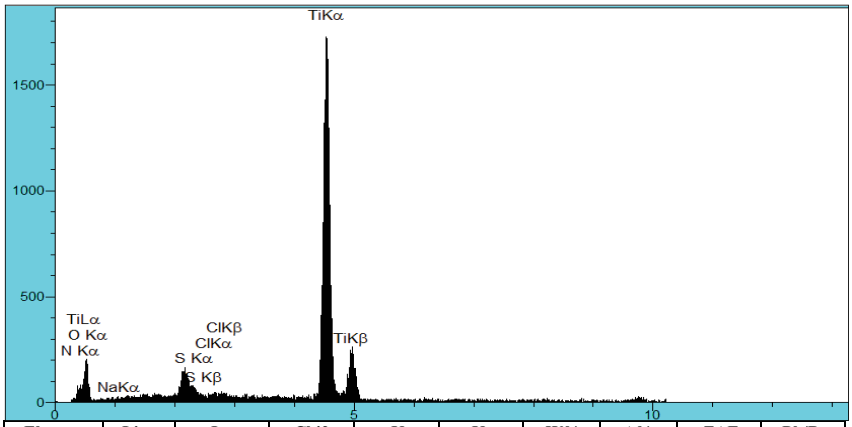

Element	Line	Int	Chi2	K	Kr	W%	A%	ZAF	Pk/Bg
C	K	1.11	1.3536	0.0034	0.0019	0.56	1.09	0.3301	4.59
N	K	23.86	1.3760	0.0943	0.0515	9.07	15.12	0.5676	6.77
O	K	67.02	1.3983	0.0858	0.0468	40.25	58.76	0.1163	44.74
Na	K	1.03	0.3352	0.0004	0.0002	0.08	0.08	0.2764	2.09
S	K	82.41	1.8362	0.0351	0.0192	2.18	1.59	0.8794	4.01
Cl	K	4.70	1.8622	0.0022	0.0012	0.13	0.09	0.8835	2.20
Ti	K	1148.06	1.8149	0.7788	0.4249	47.73	23.27	0.8903	71.09
Total				1.0000	0.5456	100	100		

Fig. 3. Energy-dispersive X-ray spectroscopy analysis of TiO_2/SDS/DNPH nanocomposites.

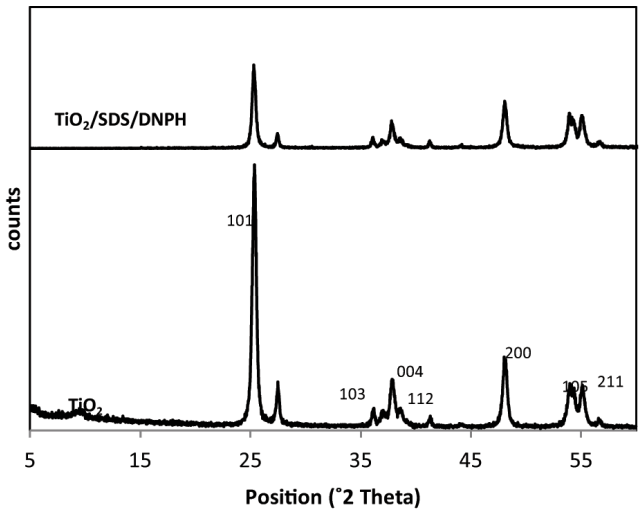

Fig. 4. X-ray diffraction patterns of TiO_2 and TiO_2/SDS/DNPH nanoparticles.

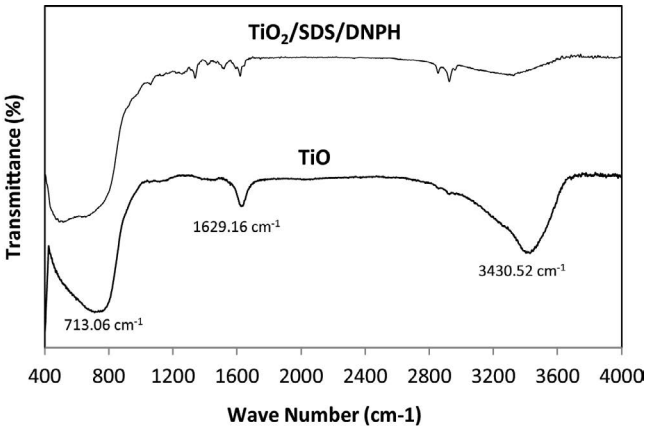

Fig. 5. Fourier-transform infrared spectra of TiO_2 and TiO_2/SDS/DNPH nanoparticles.

3,100–3,500 cm^{-1}) [32,46]. Comparison between this absorption band in TiO_2 and TiO_2/SDS/DNPH spectrums illustrates the absorption of N–H in this area which is largely overlapping with the adsorption of OH. The absorption bands at 1,345–1,640 cm^{-1} also correspond to the bending vibration of the N–H group [17,32]. Shifting the Ti–O absorption band from 713.06 to 514.84–652.57 cm^{-1} is also indicative of the composition of Ti–O with other elements during the surface modification process [17].

3.3. Study of process parameters

The optimal condition to achieve maximum pollutant removal efficiency is important in the adsorption process. Using the initial concentration of 500 mg/L for formaldehyde, a set of experiments was carried out to check the effect of various process parameters, including contact time (60–210 min), pH (4–10) and adsorbent dosage (0.5–1.5 g/L) on formaldehyde adsorption. Statistical analysis indicated that contact time and adsorbent dosage have interactive effects. Fig. 6 presents the comparison of formaldehyde uptake and the interactive effect of contact time and adsorbent dose on formaldehyde adsorption efficiency by modified and unmodified TiO_2. As expected, increasing the contact time has improved the efficiency of formaldehyde adsorption due to the increased collision chance of formaldehyde with active sites on the adsorbent [35]. Further, the rapid adsorption at the initial contact time can be attributed to the availability of the reactive site of the adsorbent [36]. As time passes due to adsorbent saturation, approaching equilibrium and decreasing formaldehyde concentration in solution, the removal rate does not change significantly [18]. The maximum adsorption efficiency achieved by unmodified TiO_2 nanoparticles was 81.8% at 135 min. The comparison of the results obtained showed that the maximum adsorption efficiency (94.6% at 135 min) obtained by modified TiO_2 was approximately 15.6% higher than the unmodified nanoparticle. This is due to the increased adsorbent surface and the high tendency of the nitrogen agent integrated with TiO_2 to absorb formaldehyde [43]. Therefore, the grafting of nano-TiO_2 with DNPH would greatly improve formaldehyde adsorption efficiency.

The pH of the solution is another important factor that should be considered in removal efficiency of formaldehyde using prepared adsorbent. The effect of pH on formaldehyde adsorption was investigated by changing pH from 4.0 to 10.0 and also 2.8 and 11.2 as axial points in the CCD design, using 0.01–0.1 M NaOH or HCl (Fig. 7a and b). The experimental results showed that the maximum formaldehyde adsorption efficiency of nano-TiO_2 was 81.8% at pH 7. At low pH, formaldehyde removal was decreased because of the competition between formaldehyde, a strong electrophile, and H^+ ions for bonding on TiO_2 nanoparticles active sites [47]. When using modified TiO_2, under acidic conditions, hydrogen ions (H^+) protonated the nitrogen-containing functional groups of the TiO_2/SDS/DNPH nanocomposites, resulting in decreased adsorption of formaldehyde by these functional groups [17]. At pH values higher than 7.0, the removal percentage decreased significantly. Indeed, in alkaline conditions some aldehydes such as formaldehyde react with hydroxide anions (OH^-) and produce alkoxide. This alkoxide lost its proton and converted into other intermediate products [17]. These compounds probably have some absorption in spectrophotometry analysis. A comparison of the obtained results showed that at pH 7 the maximum adsorption efficiency (94.6%) of modified TiO_2 was about 15.6% higher than that of unmodified nanoparticles.

The effect of nano-TiO_2 and TiO_2/SDS/DNPH nanocomposites dosage and its interaction with time on formaldehyde removal are illustrated in Fig. 6c and d. The extent of formaldehyde removal increased by increasing the adsorbent dosage. Since the change in adsorption efficiency with adsorbent dosage is incremental, the formaldehyde adsorption process on TiO_2/SDS/DNPH has not reached equilibrium. Therefore, a higher adsorption efficiency is possible by using more amounts of adsorbent. Using unmodified nano-TiO_2, the highest adsorption efficiency was 81.8% with 1.7 g/L of adsorbent, respectively. It is noteworthy that due to their high surface-to-volume ratio, nanoparticles have a high adsorption capacity, so favorable results can be achieved in pollutant elimination using very low amounts of nanoadsorbents. According to the Fig. 6c and d, adsorbent dosage and time

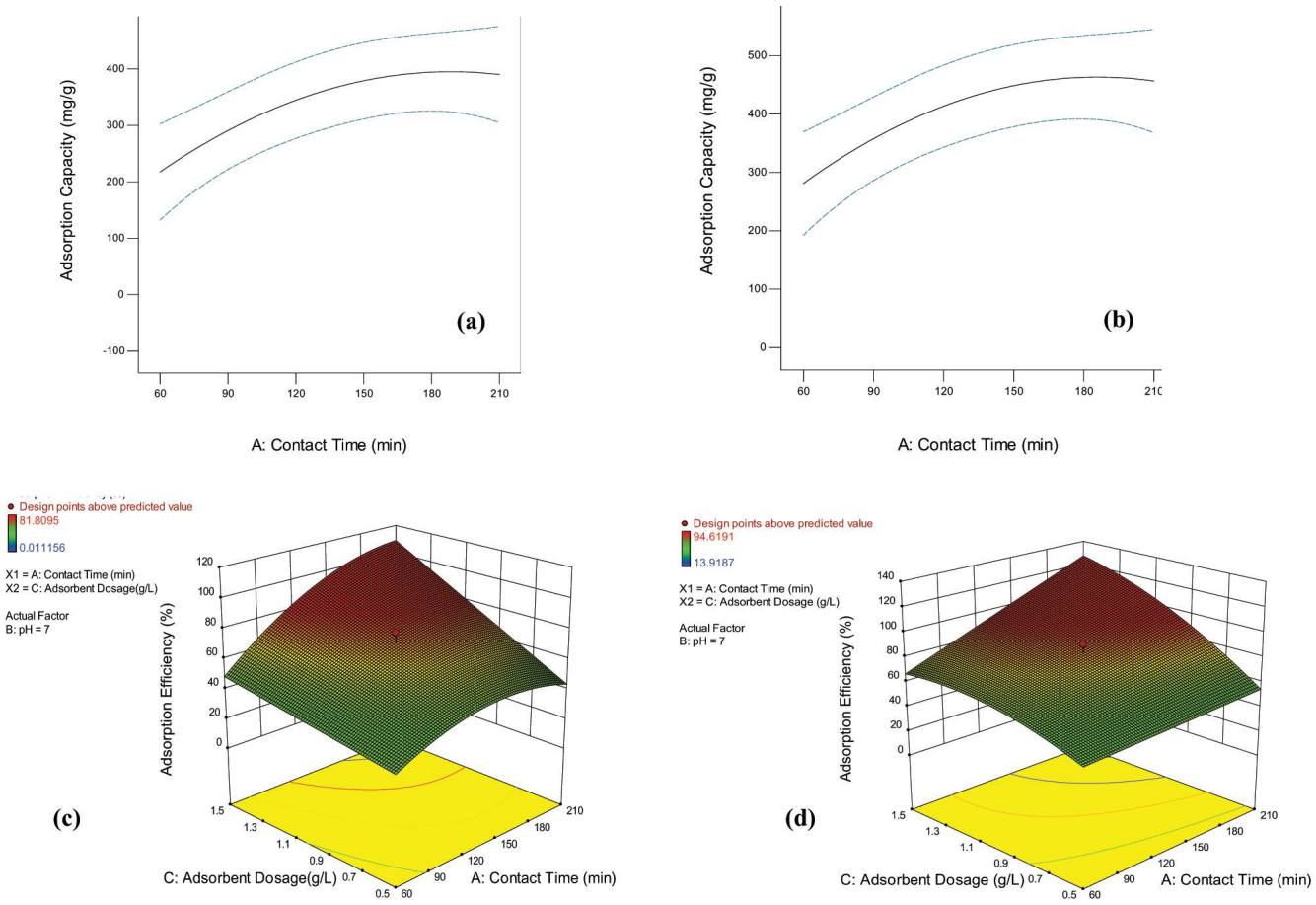

Fig. 6. Effect of contact time on adsorption capacity of (a) TiO_2 and (b) TiO_2/SDS/DNPH nanoparticles. Interactive effects of contact time and adsorbent dosage on adsorption efficiency by (c) TiO_2 and (d) TiO_2/SDS/DNPH nanoparticles.

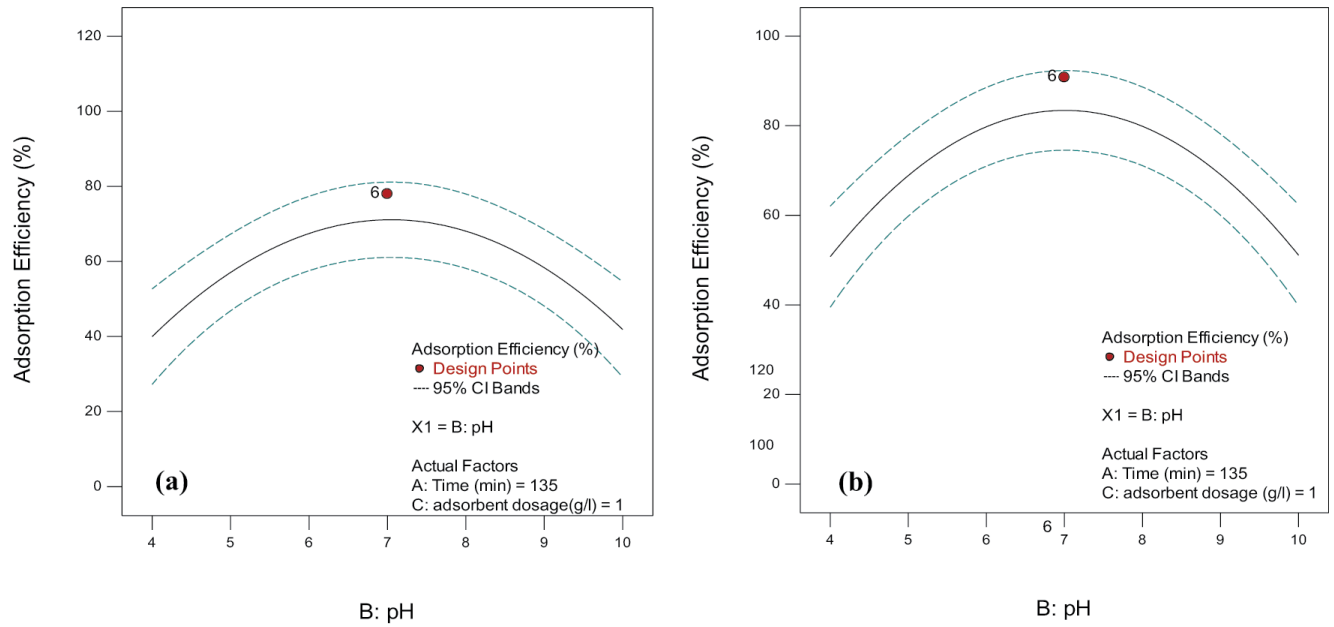

Fig. 7. Effect of pH on adsorption efficiency of (a) TiO_2 nanoparticles and (b) TiO_2/SDS/DNPH nanocomposites.

have an incremental effect on adsorption efficiency. However, according to the *F*-values obtained in the statistical analysis, the effect of the adsorbent dosage on the adsorption performance was much greater than that of time. The maximum formaldehyde adsorption efficiency of TiO_2/SDS/DNPH nanocomposites was 94.6%, which was higher than the unmodified TiO_2 with the same adsorbent dosage. This improvement in removal performance can be attributed to the formaldehyde reaction with nitrogen-containing functional groups on the surface of modified TiO_2. A possible mechanism for the formaldehyde adsorption is reaction of formaldehyde with the amine group to produce new imine group [17,48]:

$$R-NH_2+HCHO\rightarrow R-N=CH_2+H_2O \tag{4}$$

According to Eq. (4), if formaldehyde reacts with the amino groups on the surface of the TiO_2, the amount of formaldehyde adsorbed onto the modified nano-TiO_2 could increase significantly [30]. Some important aspects of the efficient removal of formaldehyde can be discussed further. First, the active hydrogen atom of the adsorbent might react with formaldehyde to form alcohol. Moreover, nitrogen atoms in the TiO_2/SDS/DNPH structure possess a partially negative charge for their strong electronegativity, while the formaldehyde carbon atom shows a slightly positive charge for its weaker electronegativity than the oxygen atom. So, the nitrogen atoms in the TiO_2/SDS/DNPH structure and carbon atom in the carbonyl of formaldehyde attract each other for the electrostatic gravitation, leading to better formaldehyde adsorption capacity onto TiO_2 [17].

3.4. Adsorption isotherms

Parameters obtained from equilibrium models can provide useful information on the sorption mechanism, surface properties, and affinity for an adsorbent [49]. The adsorption capacity for formaldehyde on the prepared TiO_2/SDS/DNPH adsorbents was tested using solutions with five varying concentrations of formaldehyde. The adsorption of formaldehyde from all these solutions was carried out under the optimum conditions obtained from the study of process parameters. The data were recorded at equilibrium conditions. Langmuir, Freundlich, and Temkin adsorption isotherms were used to describe the equilibrium characteristics of adsorption. The Langmuir isotherm is the most widely used equation that is valid for monolayer adsorption with a constant energy, and there is no transmigration of adsorbate in the plane of the adsorbent surface [50]. Its nonlinear and linear forms are expressed as:

$$q_e=\frac{q_m K_L C_e}{1+K_L C_e} \tag{5}$$

$$\frac{C_e}{q_e}=\frac{C_e}{q_{\max}}+\frac{1}{K_L q_{\max}} \tag{6}$$

Eq. (6) can be rearranged to obtain other different linearized types such as [51,52]:

$$\frac{1}{q_e}=\frac{1}{K_L q_{\max}}\frac{1}{C_e}+\frac{1}{q_{\max}} \tag{7}$$

where $q_{\max}$ is the maximum adsorption capacity at a monolayer (mg/g), C_e is the concentration of formaldehyde at equilibrium, q_e is the adsorption capacity at equilibrium (mg/g), and K_L is the Langmuir constant representing the affinity of binding sites (L/mg). A linear plot of $1/q_e$ vs. $1/C_e$ gives $q_{\max}$ and K_L. One of the essential characteristics of the Langmuir isotherm is a dimensionless constant of separation factor or equilibrium parameter, R_L, which is given by:

$$R_L=\frac{1}{1+K_L C_0} \tag{8}$$

where C_0 is the initial concentration of formaldehyde. If $0<R_L<1$, then it indicates favorable adsorption, while $R_L>1$, $R_L=1$, and $R_L=0$ indicate unfavorable, linear, and irreversible adsorption isotherms [19]. Another widely used isotherm is the empirical Freundlich equation, which is based on sorption on a heterogeneous surface [53]. The heat of adsorption decreases in magnitude with increasing extent of adsorption. If the decline in heat of adsorption is logarithmic, it implies that adsorption sites are distributed exponentially with respect to an adsorption energy that differs between groups of adsorption sites. The Freundlich equation is known as:

$$q_e=K_F C_e^{1/n} \tag{9}$$

So, the linear form of the Freundlich isotherm is:

$$\ln q_e=\ln K_F+\frac{1}{n}\ln C_e \tag{10}$$

where K_F and n are the Freundlich constants representing sorption capacity (mg/g) and intensity, respectively. K_F and n can be determined from a linear plot of $\ln q_e$ against $\ln C_e$ [49]. Freundlich parameter n relates to the surface heterogeneity; values of $n>1$ representing favorable adsorption conditions; while $n<1$ indicates that adsorbate is unfavorably adsorbed on an adsorbent [54]. The Temkin isotherm considered the effects of indirect adsorbate/adsorbent interactions on adsorption isotherms [55]. The heat of adsorption of all the molecules in the layer would decrease linearly with coverage due to adsorbate/adsorbent interaction [19,56]. The Temkin isotherm is given as:

$$q_e=B_T\ln\left(K_T C_e\right) \tag{11}$$

With linearized form as:

$$q_e=B_T+K_T\ln C_e \tag{12}$$

where K_T is the constant of Temkin isotherm (L/g) and B_T is the Temkin isotherm constant related to the heat of adsorption (kJ/mol). The linear plots of these isotherms are shown in Fig. 8. The parameters of the three isotherms are listed in Table 2.

Based on the calculated correlation coefficients, the Langmuir isotherm was more suitable for the estimation of formaldehyde removal from the aqueous solution using TiO_2/SDS/DNPH with a maximum adsorption capacity of 51.282 mg/g (Fig. 8a). The $q_{\max}$ parameter of this model could be the representative adsorption capacity of the adsorbents.

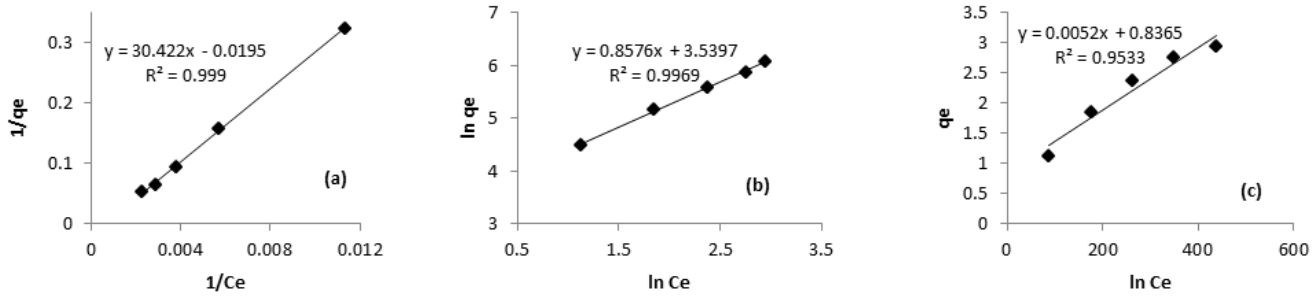

Fig. 8. Equilibrium isotherms for adsorption of formaldehyde onto TiO_2/SDS/DNPH nanocomposites: (a) Langmuir, (b) Freundlich, and (c) Temkin.

Table 2
Isotherm parameters for formaldehyde adsorption on TiO_2/SDS/DNPH

Langmuir parameters				Freundlich parameters			Temkin parameters		
q_{max} (mg/g)	K_L (L/mg)	R_L	R^2	n	K_F (mg/g)	R^2	K_T (L/g)	B_T (kJ/mol)	R^2
51.282	6.41E-04	0.757–0.939	0.999	1.166	34.456	0.9969	0.0052	0.8365	0.9533

As mentioned in the FTIR result, formaldehyde can be adsorbed on the surface sites of an adsorbent by interacting with amine groups on the adsorbent. Thus, the q_{max} of the sample depended on the number of amine groups or the length of the amino chain [54]. The R_L values in the study were found to be 0.757–0.939, indicating that this adsorption process is favorable. The favorable Langmuir isotherm is also tested further from its R_L which is favorable as in the case for formaldehyde adsorption on TiO_2/SDS/DNPH. The basic assumption of Langmuir isotherms is that adsorption takes place at specific homogeneous sites and a monolayer coverage of the adsorbate on the outer surface of the adsorbent will be created, so once formaldehyde occupies this site, no further adsorption can take place at this site. It also assumes that intermolecular forces decrease rapidly with distance from the adsorption surface [19]. The Freundlich model (Fig. 8b) was investigated for adsorption capacity (K_F) and adsorption intensity (n). The K_F value calculated from the intercept was 34.456 mg/g, showing that formaldehyde is highly adsorbed on modified TiO_2 nanoparticles and the easy separation of formaldehyde from the aqueous solution. The adsorption intensity (n) of formaldehyde on the adsorbents showed values greater than unity, representing favorable adsorption conditions [54]. The Temkin adsorption isotherm was used to estimate the adsorption potentials of formaldehyde adsorbents (Fig. 8c). The high value of B_T (0.8365 kJ/mol) related to the heat of formaldehyde adsorption onto the adsorbent indicates a strong interaction between formaldehyde molecules and the surface sites on the pores of the adsorbent.

3.5. Adsorption kinetics

The study of adsorption kinetics is important in order to determine the uptake rate of the adsorbate at the solid-phase interface [19]. Adsorption kinetic experiments were carried out at an initial concentration of 500 mg/L as a function of contact time to determine the necessary equilibrium time

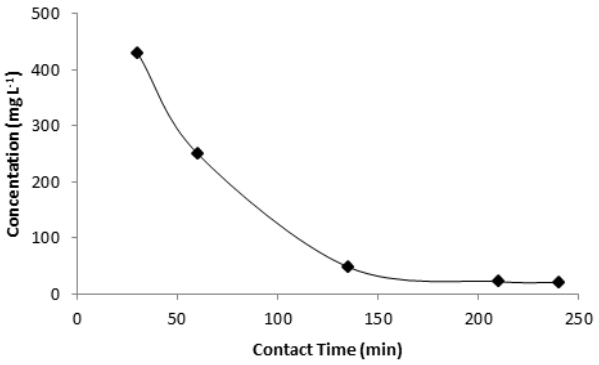

Fig. 9. Formaldehyde concentration as a function of contact time for adsorption onto TiO_2/SDS/DNPH nanocomposites at initial concentration of 500 mg/L and 1.1 g/L of adsorbent at pH 7.4 (the optimum conditions).

of adsorption. It was found that the adsorption rate is rapid at the initial stages and reaches equilibrium after 245 min (Fig. 9).

Pseudo-first-order, pseudo-second-order, and intraparticle diffusion models were used to describe the adsorption kinetic data. The pseudo-first-order equation of Lagergren and its integrated form are given by:

$$\frac{dq_t}{dt} = K_1\left(q_e - q_t\right) \tag{13}$$

$$\ln\left(q_e - q_t\right) = \ln q_e - \frac{k_1}{2.303}t \tag{14}$$

The pseudo-second-order equation assumes that the rate-limiting step is chemisorption in nature. The mechanism may involve valence forces by sharing or by the exchange of electrons between the adsorbent and the adsorbate. This kinetic equation and its integrated form are given as follows:

$$\frac{dq_t}{dt} = K_2\left(q_e - q_t\right)^2 \quad (15)$$

$$\frac{t}{q_t} = \frac{1}{k_2 q_e^2} + \frac{t}{q_e} \quad (16)$$

where q_e and q_t are the adsorption capacities of formaldehyde (mg/g) at equilibrium and time t, respectively; k_1 (min^{-1}) and k_2 (g/mg·min) are the rate constants of first-order and second-order, respectively. According to Eq. (14), the plot of $\ln(q_e - q_t)$ vs. t gives a straight line with a slope of $-k_1$ and an intercept of $\ln q_e$. From Eq. (16), the plot of t/q_t vs. t gives a straight line with a slope of $1/q_e$ and an intercept of $1/(k_2 \cdot q_e^2)$. The rate constant of intraparticle diffusion K_{diff} was calculated by using the following equation:

$$q_t = K_{diff} t^{1/2} + C \quad (17)$$

where q_t) mg/g) is the amount adsorbed at time t and $t^{1/2}$. The adsorption kinetic plots are shown in Fig. 10, and the related parameters calculated from the three models are listed in Table 3. The values of the correlation coefficients (R^2) clearly indicated that the adsorption kinetics closely followed the pseudo-first-order model rather than other models. Moreover, the calculated equilibrium adsorption capacity value, $q_{e,cal}$, was closer to the experimental value of $q_{e,exp}$ in the pseudo-first-order model.

3.6. Adsorption thermodynamics

Three important thermodynamic parameters that should be considered and determined in adsorption processes are standard Gibbs free energy ($\Delta G°$), standard enthalpy ($\Delta H°$), and standard entropy ($\Delta S°$) [57,58]. Values of ($\Delta H°$) and ($\Delta S°$) were calculated by using the following equation:

$$\ln K_d = \frac{\Delta S°}{R} - \frac{\Delta H°}{RT} \quad (18)$$

$$K_d = \frac{q_e}{C_e} \quad (19)$$

where R is the ideal gas constant 8.314 (J/mol·K), T is the temperature of the solution, and K_d is the ratio of the amount of the adsorbed formaldehyde to that of the solution [59]. $\Delta H°$ and $\Delta S°$ were derived from the slope and intercept of the linear equation of $\ln K_d$ as a function of $1/T$. Also, $\Delta G°$ were calculated by using the following equation:

$$\Delta G° = -RT \ln K_L \quad (20)$$

According to the adsorption thermodynamics, $\Delta H°$, $\Delta G°$, and $\Delta S°$ were calculated as –26.1, –5.6, and –63.2 (kJ/mol), respectively [60]. Negative values obtained for $\Delta H°$, $\Delta G°$, and $\Delta S°$ show that the reaction is exothermic and spontaneous at room temperature, which has been reported previously in other studies [61–63].

3.7. Regeneration of adsorbent

In multiple cycle adsorption–desorption tests, formaldehyde adsorption was performed with an initial formaldehyde concentration of 500 ppm and 1.1 g/L of TiO_2/SDS/DNPH at pH 7.4 (the optimum conditions). The results indicated that the adsorption efficiency decreased after each adsorption–desorption cycle for all washing solutions. This decrease was very slight for the NaOH solution. There was no significant difference during the five adsorption–regeneration cycles (Fig. 11). The first regenerated TiO_2/SDS/DNPH nanocomposites could remove 96% formaldehyde (only 0.21% less than the fresh adsorbent) and 93.7% after

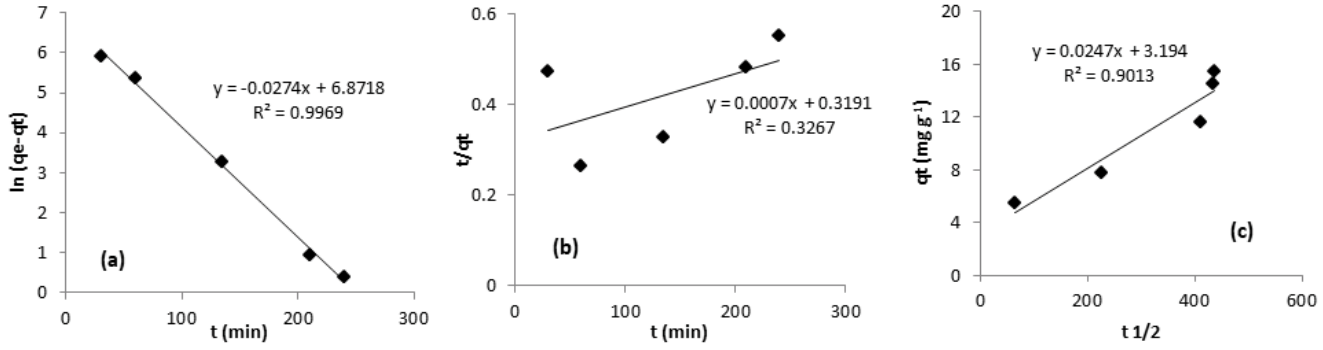

Fig. 10. Adsorption kinetic of formaldehyde onto TiO_2/SDS/DNPH nanocomposites: (a) pseudo-first-order kinetic, (b) pseudo-second-order kinetic and (c) intraparticle diffusion.

Table 3
Kinetic model parameters for adsorption of formaldehyde onto adsorbent at initial concentration of 500 mg/L

C_0 (mg/L)	$q_{e,exp}$ (mg/g)	Pseudo-first-order			Pseudo-second-order			Intraparticle diffusion		
		q_{e1} (mg/g)	k_1 (min^{-1})	R^2	q_{e2} (mg/g)	k_2 (g/mg·min)	R^2	K_{id} (mg/g·min$^{0.5}$)	C	R^2
500	439.0909	964.683	0.063	0.9969	1,428.57	1.535E-06	0.3267	0.0247	3.194	0.9013

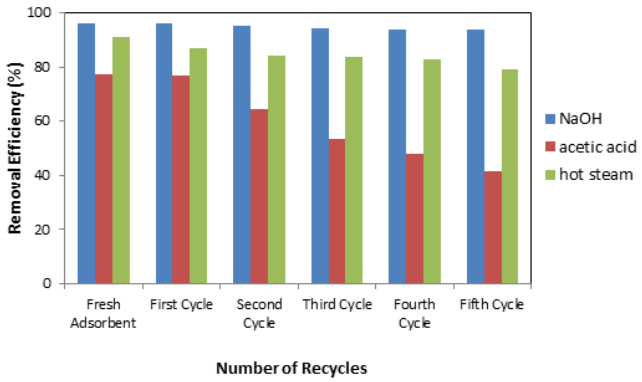

Fig. 11. Formaldehyde removal efficiency of TiO_2/SDS/DNPH adsorbent (at optimal conditions) over five regeneration cycles.

Table 4
Predicted and experimental optimum conditions for formaldehyde removal by TiO_2/SDS/DNPH.

Optimum conditions	Predicted	Experimental
Contact time (min)	183.290	183.290
pH	7.424	7.424
Absorbent dosage (g/L)	1.100	1.100
Adsorption efficiency (%):	99.904	3.7
Error (%)	96.2	1.1

regeneration 5 times. Therefore, the obtained results confirm that the majority of adsorbent can be recycled.

3.7. Optimum conditions

Analysis of the results by Design–Expert software showed that the quadratic model was statistically well matched to the obtained data for formaldehyde removal by TiO_2 nanoparticles before and after grafting with DNPH. Design–Expert software has been used to determine the optimal elimination conditions within the tested range. The predicted and experimental optimum conditions for formaldehyde removal by TiO_2/SDS/DNPH together with the maximum adsorption value, are illustrated in Table 4.

4. Conclusions

The functionalized TiO_2/SDS/DNPH nanocomposites developed with an average size of 70–80 nm were successfully used for formaldehyde removal from water up to 96.2% under optimum conditions. EDX and FTIR analysis confirmed the formation of TiO_2/SDS/DNPH and the presence of N–H functional groups on the surface of the adsorbent. The adsorption efficiency of modified TiO_2 for formaldehyde was found to be 15.65% higher than that of unmodified TiO_2. Therefore, the combination of nano-TiO_2 with DNPH would greatly improve formaldehyde adsorption efficiency. According to experimental data, formaldehyde adsorption by TiO_2/SDS/DNPH followed the Langmuir isotherm. Adsorption of formaldehyde onto TiO_2/SDS/DNPH obeyed the pseudo-first-order kinetic model at initial concentration of 500 mg/L. According to the adsorption thermodynamics, $\Delta H°$, $\Delta G°$, and $\Delta S°$ were calculated as –26.1, –5.6, and –63.2 (kJ/mol), respectively, showing that the reaction is exothermic and spontaneous at room temperature. The optimum conditions predicted for maximum formaldehyde removal by TiO_2/SDS/DNPH nanocomposites were adsorbent dosage 1.100 g/L, pH 7.424 and the contact time 183.290 min. It was concluded that the surface-modified nano-TiO_2 can be considered a new and efficient agent to remove formaldehyde from water.

Acknowledgment

The authors sincerely thank the officials at Islamic Azad University, Quchan Branch, for their financial support and the provision of laboratory equipment.

References

[1] Sh. Ebrahimi, M. Borghei, Formaldehyde biodegradation using an immobilized bed aerobic bioreactor with pumice stone as a support, Sci. Iran., 18 (2011) 1372–1376.
[2] L. Zhang, Formaldehyde: Exposure, Toxicity and Health Effects, Royal Society of Chemistry, 2018.
[3] L. Zhang, Chapter 1: Introduction to Formaldehyde, Issues in Toxicology, Royal Society of Chemistry, 2018.
[4] K. Veenagayathri, N. Vasudevan, Biodegradation of formaldehyde under saline conditions by a moderately halophilic bacterial consortium, Curr. World Environ.: An Int. Res. J. Environ. Sci., 5 (2010) 31–38.
[5] C. Jarusutthirak, K. Sangsawang, S. Mattaraj, R. Jiraratananon, Treatment of formaldehyde-containing wastewater using membrane bioreactor, J. Environ. Eng., 138 (2012) 265–271.
[6] P. Kowalik, Chemical Pretreatment of Formaldehyde Wastewater by Selected Advanced Oxidation Processes (AOPs), 2011.
[7] K. Raja Priya, S. Sandhya, K. Swaminathan, Kinetic analysis of treatment of formaldehyde containing wastewater in UAFB reactor, J. Chem. Eng., 148 (2009) 212–216.
[8] A. Hidalgo, A. Lopategi, M. Prieto, J.L. Serra, M.J. Llama, Formaldehyde removal in synthetic and industrial wastewater by *Rhodococcus erythropolis* UPV-1, Appl. Microbiol. Biotechnol., 58 (2002) 260–264.
[9] J. Li, X. Wang, G. Zhao, C. Chen, Z. Chai, A. Alsaedi, T. Hayat, X. Wang, Metal–organic framework-based materials: superior adsorbents for the capture of toxic and radioactive metal ions, Chem. Soc. Rev., 47 (2018) 2322–2356.
[10] X. Li, Y. Liu, C. Zhang, T. Wen, L. Zhuang, X. Wang, G. Song, D. Chen, Y. Ai, T. Hayat, Porous Fe_2O_3 microcubes derived from metal organic frameworks for efficient elimination of organic pollutants and heavy metal ions, J. Chem. Eng., 336 (2018) 241–252.
[11] L. Vidhya, M. Dhandapani, K. Shanthi, S. Kamala-Kannan, Removal of Cr(VI) from aqueous solution using coir pith biochar – an eco-friendly approach, Indian J. Chem. Technol., 25 (2018) 266–273.
[12] R.-M. Naik, S. Ratan, I. Singh, Use of orange peel as an adsorbent for the removal of Cr(VI) from its aqueous solution, Indian J. Chem. Technol., 25 (2018) 300–305.
[13] R. Sudha, P. Premkumar, Comparative studies on the removal of chromium(VI) from aqueous solutions using raw and modified *Citrus limettioides* peel, Indian J. Chem. Technol., 25 (2018), doi: 10.56042/ijct.v25i3.11706.
[14] M. Salman, M. Athar, U. Shafique, R. Rehman, Removal of formaldehyde from aqueous solution by adsorption on kaolin and bentonite: a comparative study, Turk. J. Eng. Environ. Sci., 36 (2012) 263–270.
[15] D.-Y. Ryu, T. Shimohara, K. Nakabayashi, J. Miyawaki, J.-I. Park, S.-H. Yoon, Urea/nitric acid co-impregnated pitch-based activated carbon fiber for the effective removal of formaldehyde, J. Ind. Eng. Chem., 80 (2019) 98–105.

[16] C.-J. Na, M.-J. Yoo, D.C. Tsang, H.W. Kim, K.-H. Kim, High-performance materials for effective sorptive removal of formaldehyde in air, J. Hazard. Mater., 366 (2019) 452–465.
[17] A. Afkhami, H. Bagheri, T. Madrakian, Alumina nanoparticles grafted with functional groups as a new adsorbent in efficient removal of formaldehyde from water samples, Desalination, 281 (2011) 151–158.
[18] Z. Hejri, A.A. Seifkordi, A. Ahmadpour, S.M. Zebarjad, A. Maskooki, Biodegradable starch/poly(vinyl alcohol) film reinforced with titanium dioxide nanoparticles, Int. J. Miner. Metall. Mater., 20 (2013) 1001–1011.
[19] Z. Ghasemi, A. Seif, T.S. Ahmadi, B. Zargar, F. Rashidi, G.M. Rouzbahani, Thermodynamic and kinetic studies for the adsorption of Hg(II) by nano-TiO_2 from aqueous solution, Adv. Powder Technol., 23 (2012) 148–156.
[20] E. Petala, M. Baikousi, M.A. Karakassides, G. Zoppellaro, J. Filip, J. Tuček, K.C. Vasilopoulos, J. Pechoušek, R. Zbořil, Synthesis, physical properties and application of the zero-valent iron/titanium dioxide heterocomposite having high activity for the sustainable photocatalytic removal of hexavalent chromium in water, Phys. Chem. Chem. Phys., 18 (2016) 10637–10646.
[21] Y. Lu, P.R. Chang, P. Zheng, X. Ma, Rectorite–TiO_2–Fe_3O_4 composites: assembly, characterization, adsorption and photodegradation, Chem. Eng. J., 255 (2014) 49–54.
[22] S. Khosroyar, A. Arastehnodeh, Improving hydrophilic and antimicrobial properties of membrane by adding nanoparticles of titanium dioxide and copper oxide, Membr. Water Treat., 9 (2018) 481–487.
[23] Y.H. Okour, S.S. Ahmed, Recovery of Titania from Waste-Sludge of Majmaah Water Treatment Plant, The Third International Conference on Water, Energy and Environment (ICWEE), AUS, American University of Sharjah, UAE, 2015.
[24] S. Mehta, S. Patel, Recovery of titania from the bauxite sludge, J. Am. Chem. Soc., 73 (1951) 226–227.
[25] S.M. Khezri, A.A. Bloorchian, Titanium dioxide extraction from paint sludge of automotive industry case study: paint sludge of saipa paint shop, Environ. Eng. Manage. J., 8 (2009), doi: 10.30638/eemj.2009.021.
[26] K.-h. Lim, B.-h. Shon, Metal components (Fe, Al, and Ti) recovery from red mud by sulfuric acid leaching assisted with ultrasonic waves, Int. J. Emerg. Technol. Adv. Eng., 5 (2015) 25–32.
[27] X. Xie, L. Gao, Effect of crystal structure on adsorption behaviors of nanosized TiO_2 for heavy-metal cations, Curr. Appl. Phys., 9 (2009) S185–S188.
[28] S. Suriyaraj, T. Vijayaraghavan, P. Biji, R. Selvakumar, Adsorption of fluoride from aqueous solution using different phases of microbially synthesized TiO_2 nanoparticles, J. Environ. Chem. Eng., 2 (2014) 444–454.
[29] S. Sun, J. Ding, J. Bao, C. Gao, Z. Qi, C. Li, Photocatalytic oxidation of gaseous formaldehyde on TiO_2: an *in-situ* DRIFTS study, Catal. Lett., 137 (2010) 239–246.
[30] H. Rong, Z. Liu, Q. Wu, D. Pan, J. Zheng, Formaldehyde removal by Rayon-based activated carbon fibers modified by P-aminobenzoic acid, Cellulose, 17 (2010) 205–214.
[31] R. Zhu, R. Chen, Y. Duo, S. Zhang, D. Xie, Y. Mei, An industrial scale synthesis of adipicdihydrazide (ADH)/polyacrylate hybrid with excellent formaldehyde degradation performance, Polymers, 11 (2019) 86, doi: 10.3390/polym11010086.
[32] S. Sobhanardakani, R. Zandipak, 2,4-Dinitrophenylhydrazine functionalized sodium dodecyl sulfate-coated magnetite nanoparticles for effective removal of Cd(II) and Ni(II) ions from water samples, Environ. Monit. Assess., 187 (2015) 412, doi: 10.1007/s10661-015-4635-y.
[33] M. Danesh-khorasgani, H. Faghihian, M.H. Givianrad, P. Aberoomand-Azar, M. Saber-Tehrani, Synthesis and application of a novel mesoporous SBA-15 sorbent functionalized by 2,4 dinitrophenylhydrazine (DNPH) for simultaneous removal of Pb(II), Cr(III), Cd(II) and Co(II) from aqueous solutions: experimental design, kinetic, thermodynamic, and isotherm aspects, Adv. Powder Technol., 33 (2022) 103201, doi: 10.1016/j.apt.2021.07.010.
[34] M. Zarei, A. Hasani, Z. Hejri, Synthesis and characterization of biodegradable and antibacterial coverage based on *Aloe vera*/nanochitosan for bread packaging, J. Nanomater., 11 (2019) 119–130.
[35] Z. Hejri, A. Hasani, A. Davoudi Rad, Removal of Reactive Red 120 azo dye from aqueous solution with magnetic nanoparticles coated with chitosan, J. Appl. Chem., 15 (2020) 185–204.
[36] A. Hasani, M. Defe Jafari, Z. Hejri, M. Omidvar, Magnetic activated carbon synthesis to reduce COD from the wastewater of Parsian Khavaran fibers factory using hybrid system of adsorption and membrane, J. Appl. Chem., 14 (2019) 89–102.
[37] T. Nash, The colorimetric estimation of formaldehyde by means of the Hantzsch reaction, Biochem. J., 55 (1953) 416–421.
[38] T. Alsawy, E. Rashad, M. El-Qelish, R.H. Mohammed, A comprehensive review on the chemical regeneration of biochar adsorbent for sustainable wastewater treatment, npj Clean Water, 5 (2022) 29, doi: 10.1038/s41545-022-00172-3.
[39] G. Kianpour, R. Bagheri, A. Pourjavadi, H. Ghanbari, Synergy of titanium dioxide nanotubes and polyurethane properties for bypass graft application: excellent flexibility and biocompatibility, Mater. Des., 215 (2022) 110523, doi: 10.1016/j.matdes.2022.110523.
[40] D.L. Liao, B.Q. Liao, Shape, size and photocatalytic activity control of TiO_2 nanoparticles with surfactants, J. Photochem. Photobiol., A, 187 (2007) 363–369.
[41] A. Kumar, P. Choudhary, A. Kumar, P.H.C. Camargo, V. Krishnan, Recent advances in plasmonic photocatalysis based on TiO_2 and noble metal nanoparticles for energy conversion, environmental remediation, and organic synthesis, Small, 18 (2022) 2101638, doi: 10.1002/smll.202101638.
[42] Z. Zhou, M. Wei, G. Yang, W. Du, F. Peng, Y. Fang, Y. Liu, S. Zhang, R. Qiu, Photoinduced electron-rich CuNi@C/TiO_2 catalyst for highly efficient hydrogen production from formaldehyde aqueous solution, J. Alloys Compd., 936 (2022) 168360, doi: 10.1016/j.jallcom.2022.168360.
[43] C. Li, M. Gu, M. Gao, K. Liu, X. Zhao, N. Cao, J. Feng, Y. Ren, T. Wei, M. Zhang, N-doping TiO_2 hollow microspheres with abundant oxygen vacancies for highly photocatalytic nitrogen fixation, J. Colloid Interface Sci., 609 (2022) 341–352.
[44] A. León, P. Reuquen, C. Garín, R. Segura, P. Vargas, P. Zapata, P.A. Orihuela, FTIR and Raman characterization of TiO_2 nanoparticles coated with polyethylene glycol as carrier for 2-methoxyestradiol, Appl. Sci., 7 (2017) 49, doi: 10.3390/app7010049.
[45] S. Bagheri, K. Shameli, S.B. Abd Hamid, Synthesis and characterization of anatase titanium dioxide nanoparticles using egg white solution via sol–gel method, J. Chem., 2013 (2013) 848205, doi: 10.1155/2013/848205.
[46] T. Uma Devi, N. Lawrence, R. Ramesh Babu, K. Ramamurthi, G. Bhagavannarayana, Structural and optical characterization studies on 2,4-dinitrophenylhydrazine single crystal, Int. J. Miner. Metall. Mater., 9 (2010) 321–330.
[47] Z. Hejri, M. Hejri, M. Omidvar, S. Morshedi, A novel nanocomposite as adsorbent for formaldehyde removal from aqueous solution, Adv. Nano Res., 8 (2020) 1–11.
[48] Y. Le, D. Guo, B. Cheng, J. Yu, Bio-template-assisted synthesis of hierarchically hollow SiO_2 microtubes and their enhanced formaldehyde adsorption performance, Appl. Surf. Sci., 274 (2013) 110–116.
[49] M. Bagheri, M. Nasiri, A. Talaiekhozani, I. Abedi, Equilibrium isotherms of formaldehyde elimination from the aqueous solutions containing natural adsorbents of rice bran and the resulting ashes, J. Hum. Environ. Health Promot., 4 (2018) 87–93.
[50] Z. Wang, M. Zhong, L. Chen, Coal-based granular activated carbon loaded with MnO_2 as an efficient adsorbent for removing formaldehyde from aqueous solution, Desal. Water Treat., 57 (2016) 13225–13235.
[51] Y.-T. Huang, M.-C. Shih, Effect of linearized expressions of Langmuir equations on the prediction of the adsorption of methylene blue on rice husk, Int. J. Sci. Res. Publ., 6 (2016) 549–554.

[52] N. Benderdouche, B. Bestani, M. Hamzaoui, The use of linear and nonlinear methods for adsorption isotherm optimization of basic green 4-dye onto sawdust-based activated carbon, J. Mater. Environ. Sci., 9 (2018) 1110–1118.
[53] B. Van der Bruggen, Freundlich Isotherm, Encyclopedia of Membranes, 2015.
[54] S. Srisuda, B. Virote, Adsorption of formaldehyde vapor by amine-functionalized mesoporous silica materials, J. Environ. Sci., 20 (2008) 379–384.
[55] K.H. Chu, Revisiting the Temkin isotherm: dimensional inconsistency and approximate forms, Ind. Eng. Chem. Res., 60 (2021) 13140–13147.
[56] S. Salvestrini, L. Ambrosone, F.-D. Kopinke, Some mistakes and misinterpretations in the analysis of thermodynamic adsorption data, J. Mol. Liq., 352 (2022) 118762, doi: 10.1016/j.molliq.2022.118762.
[57] P. Saha, S. Chowdhury, Insight into adsorption thermodynamics, Thermodynamics, 16 (2011) 349–364.
[58] E.C. Lima, A. Hosseini-Bandegharaei, J.C. Moreno-Piraján, I. Anastopoulos, A critical review of the estimation of the thermodynamic parameters on adsorption equilibria. Wrong use of equilibrium constant in the Van't Hoof equation for calculation of thermodynamic parameters of adsorption, J. Mol. Liq., 273 (2019) 425–434.
[59] H.N. Tran, Improper estimation of thermodynamic parameters in adsorption studies with distribution coefficient K_d (q_e/C_e) or Freundlich constant (K_F): considerations from the derivation of dimensionless thermodynamic equilibrium constant and suggestions, Adsorpt. Sci. Technol., 2022 (2022) 5553212, doi: 10.1155/2022/5553212.
[60] H.N. Tran, E.C. Lima, R.-S. Juang, J.-C. Bollinger, H.-P. Chao, Thermodynamic parameters of liquid–phase adsorption process calculated from different equilibrium constants related to adsorption isotherms: a comparison study, J. Environ. Chem. Eng., 9 (2021) 106674, doi: 10.1016/j.jece.2021.106674.
[61] B. Kakavandi, A. Esrafili, A. Mohseni-Bandpi, A. Jonidi Jafari, R. Rezaei Kalantary, Magnetic Fe_3O_4@C nanoparticles as adsorbents for removal of amoxicillin from aqueous solution, Water Sci. Technol., 69 (2014) 147–155.
[62] D. Pereira, M.V. Gil, V.I. Esteves, N.J. Silva, M. Otero, V. Calisto, Ex-situ magnetic activated carbon for the adsorption of three pharmaceuticals with distinct physicochemical properties from real wastewater, J. Hazard. Mater., 443 (2023) 130258, doi: 10.1016/j.jhazmat.2022.130258.
[63] J. Barasarathi, P.S. Abdullah, E.C. Uche, Application of magnetic carbon nanocomposite from agro-waste for the removal of pollutants from water and wastewater, Chemosphere, 305 (2022) 135384, doi: 10.1016/j.chemosphere.2022.135384.